Magnetic Resonant Pulsed Pumping of Rubidium

by

Adam Newton Wright

Submitted in Partial Fulfillment of the
Requirements for the Degree

Bachelor of Arts

Supervised by
Dr. Micheala Kleinert

Department of Physics

Willamette University, College of Liberal Arts
Salem, Oregon

2017

Presentations and Publications

blahblah

Acknowledgments

Thanks to everyone!

Abstract

My abstract goes here.

Table of Contents

List of Tables

List of Figures

1 Introduction

In 1609, Galileo Galilei used a device of two lenses at the sky, seeing for the first time with magnification the imperfections on the moon, small objects orbiting Jupiter, and even the phases of Venus [NAS03] [Obs09]. With observations from this crude contraption, Galileo showed that Venus was orbiting the sun. This evidence supported the theoretical model of a heliocentric universe, proposed in the sixteenth century by Nicolaus Copernicus and expounded upon by Johannes Kepler in the next century [JH01]. As time progressed, inquisitive minds began to wonder what else could be discovered with the power of magnification. Telescopes, as they would be coined, began a rapid period of advancement. Lenses were made larger in diameter in order to view fainter objects. Optical components were fabricated with less imperfection allowing for better resolution. Curvature and indices of refraction of lenses were exploited, allowing for varying degrees of magnification. Achromatic, aspheric, and cylindrical lenses were created, ridding telescopes of significant aberrations. By the late twentieth century, telescopes were as optically perfect as they could be; no advancements in optics would allow them to see with greater magnification or increased resolution. However, there was a lingering problem: atmospheric distortion.

This is a distortion caused by the inhomogeneity of Earth's atmosphere. As light from astronomical bodies passes through at atmosphere, the varying levels of pressure, density, and temperature cause small distortions in the image of that object. In order to rid images of atmospheric distortions, astronomers image distance point sources, e.g. natural stars or laser guide stars, and use adaptive optics to produce a clear, distortion free image; this is discussed more thoroughly in Appendix A.

Laser guide star, artificial stars created in the upper atmosphere by interacting laser light with sodium atoms, are preferred over natural stars due to their ability to be spatially into the field of view, their brightness, and their well known spectral emission. Since the resolution of a telescope depends upon its adaptive optics system, and the adaptive optics system in turn depends upon the guide star, it is of importance to know how laser guide stars work and how they can be improved.

One important property of the laser guide star is its brightness. Its brightness can be increased by improving the intensity of the laser beam, increasing the size of the laser beam, or by using various optical techniques to increase the atom's probability of absorbing and emitting photons. One of these techniques, proposed by Kane et al [TJK14], realizes the consequences of the precession of the atom in a magnetic field and uses light pulsed at the frequency of the atom's precession frequency to increase photon return; this method was coined *magnetic resonant pulsing* (MRP).

MRP was investigated by Rampy et al. [RR10] through measurement of photon return from various CW and pulsed lasers at different latitudes. Their data show that lasers pulsed at the Larmor frequency of the atom in a magnetic field increase photon return as the laser beam nears perpendicular to the magnetic field [RR10]. This result is consistent with the theory set by Kane et al. [TJK14].

In this paper, we thoroughly test MRP under controlled conditions. We build a short-cavity dye laser pumped by a frequency-doubled Nd:VO_4 laser with a 200 kHz repetition rate and 10 ps pulse width. The dye solution is LDS-798 dissolved in methanol, capable of lasing between 765 nm and 845 nm with peak at 798 nm [Bra00]. This laser is used to perform absorption measurements on rubidium atoms[1] confined in an absorption cell and surrounded by a magnetic field. The magnetic field is created using Helmholtz coils, adjustable in both its strength and orientation with respect to the incoming laser beam and capable of producing a magnetic field of $B \approx 10\,G$.

Since the Larmor precession of an atom depends on the strength of the magnetic field, we are able to change the frequency of rubidium's precession from nearly 100 Hz to 300 kHz. Thus, we can bring the system into and out of magnetic resonant pulsing by adjusting the strength of the magnetic field while measuring the amount of light rubidium absorbs.

[1]Rubidium has similar properties to sodium, including a similar gyromagnetic ratio, magnetic moment, and Larmor precession, in addition to both being alkali metals. It was chosen over sodium in this experiment since the overall focus of this laboratory is concerned with rubidium.

2 Background

Laser guide stars (LGS)[1] are invaluable instruments in modern astronomy, allowing observations of extremely high resolution to be made even in unfavorable atmospheric conditions. An important quality of a LGS is its brightness, which affects the overall performance of the adaptive optics system, thus limiting the resolution that the telescope can achieve. However, taking advantage of the atoms precession in a magnetic field, the brightness of LGS can be increased through magnetic resonant pulsing (MRP). In this chapter, we describe the quantum theory behind LGS, magnetic resonant pulsing, second harmonic generation, and an ultrafast dye laser.

2.1 Quantum Theory of LGS

As dictated by quantum mechanics, atoms have unique, quantized energy levels. In the simplest model, the electrons in the atom can be thought of as "orbiting" the nucleus; this model is known as the *Bohr model*, proposed by Neils Bohr and Ernest Rutherford in the early nineteenth century. The electrons "orbit" in quantized radii, or shells, each of which is denoted by the principal quantum number n for $n = 1, 2, 3, \ldots$. Each value of n can have an angular momentum value of $0 \geq l < n$; thus, each shell has a $n-1$ degeneracy. In each of these shells, the electrons can also have a quantized angular momentum value, given by the orbital angular momentum number l. The orbital angular momentum is

$$l = n\hbar \tag{2.1}$$

where n is the principal quantum number and $\hbar = \frac{h}{2\pi}$ is the reduced Plank's constant. Each electron shell refers to a certain energy of the atom, and electrons

[1] LGS will refer to both the plural and singular of the word, e.g. "LGS are frequently used in modern astronomy" and "LGS systems consist of many components." Context should provide the correct form throughout reading this paper.

are free to transition between shells as long as energy is conserved during this transition[2]. As a pedagogical example, we can calculate the energy difference of an electron transitioning between shells for hydrogen using the famous Rydberg formula:

$$\Delta E = R\left(\frac{1}{n_f^2} - \frac{1}{n_i^2}\right) \tag{2.2}$$

where R is a constant, n_f is the final principal quantum number and n_i is the initial principal quantum number. Empirically, we see that atoms emit photons when the decay from from states of higher energy to those with lower energy. Knowing that the energy of a photon is

$$E = hf = \frac{hc}{\lambda} \tag{2.3}$$

where h is Planck's constant, f is the frequency of the photon, c is the speed of light in a vacuum, and λ is the wavelength of the photon, we can calculate the wavelength of light a transition would emit using this and the Rydberg formula (Equation 2.2):

$$\frac{1}{\lambda} = hcR\left(\frac{1}{n_f^2} - \frac{1}{n_i^2}\right) \tag{2.4}$$

This process is also reversible, meaning we can actually excite the atom by sending a photon of similar wavelength to the atom; the corresponding frequency of this wavelength is known as the resonant frequency. We can thus excite atoms by interacting laser light of resonant frequency with them and in turn observe the light they radiate upon decay. This is the foundation of a LGS — laser light resonant with sodium is shone onto the sodium atoms in the atmosphere, the atoms absorb this light, and then emit this light in random directions, creating a "globe" of light (See Append A).

The Bohr model however isn't completely accurate. If we look closely, we see that particles not only can have a relativistic kinetic energy but also have a quality known as spin. Spin is a quantity that all particles possess and describes the particle's intrinsic angular momentum; it takes integer or half integer values of the reduced Plank's constant. For example, electrons are spin-$\frac{1}{2}$ particles and thus have spin $S = \pm\frac{\hbar}{2}$ while photons are spin-1 with $S = \pm 1$. Spin, being a value of the intrinsic angular momentum, can couple with the *orbital* angular momentum, causing an interaction that shifts and splits the energy levels; the

[2]Other quantities, such as angular momentum, must also be conserved; these will be addressed shortly.

relativistic kinetic energy simply shifts the energy. Collectively, these corrections are known as the *fine structure* [Kib09]. These splitting follows the rule

$$\vec{J} = \vec{L} + \vec{S} \tag{2.5}$$

where $\vec{L}$ is the orbital angular momentum and $\vec{S}$ is the spin number. The values that the splitting can thus take are $|\vec{J}| = |l - s| + \cdots + |l + s|$ in integer steps. Thus, for the $l = 0$ state of particle spin-$\frac{1}{2}$, $j = |0 - \frac{1}{2}| \ldots |0 + \frac{1}{2}| = \frac{1}{2}$, indicating there only being an energy shift, and not split, for this state. However, for the $l = 1$ state, $j = |1 - \frac{1}{2}| \ldots |1 + \frac{1}{2}| = -\frac{1}{2} \ldots \frac{3}{2} = -\frac{1}{2}, \frac{1}{2}, \frac{3}{2}$, indicating a three-fold split.

We can still look even closer at the energy levels of atoms. We saw how the spin of the electron can interact with its orbital angular momentum to cause an energy split, but this spin can also interact with the spin of the nucleus, causing yet another, small[3] splitting of the energy levels. The hyperfine structure follows the rule

$$\vec{F} = \vec{J} + \vec{I} \tag{2.6}$$

where $\vec{I}$ is the nuclear spin vector. The splitting obeys $|\vec{F}| = |j - I| \ldots |j + i|$, causing degeneracy for all states with $j \neq 0$ and $I \neq 0$.

Finally, we can discuss the last relevant correction. If we consider the atom to be in a magnetic field, we get another splitting known as the *Zeeman structure*. This comes from the magnetic field interacting with the vector $\vec{F}$, causing a precession of this vector along the axis of the magnetic field. The energy shift follows the equation

$$\Delta E = \mu_0 m_j g_F B \tag{2.7}$$

where μ_0 is the permeability of free space, m_j is the z-component of the total angular momentum, g_F is the Lande g-factor,[4] and B is the magnetic field. The

[3]For hydrogen, these shifts are on the order of millionths of an eV [Fey65]; compared with the ionization energy of 13.6 eV, this is quite small.

[4]The Lande g-factor is a particular g-factor (see Section 2.2 for an introduction to the g-factor) that accounts for both the spin and orbital angular momentum of the particle. It is described mathematically as

$$g_F = g_J \frac{F(F+1) - I(I+1) + J(J+1)}{2F(F+1)} + g_I \frac{F(F+1) + I(I+1) - J(J+1)}{2F(F+1)} \tag{2.8}$$

where $g_{J,I}$ are the Lande g-factors for the those particular quantum values, and F, J, I are the quantum values discussed earlier.

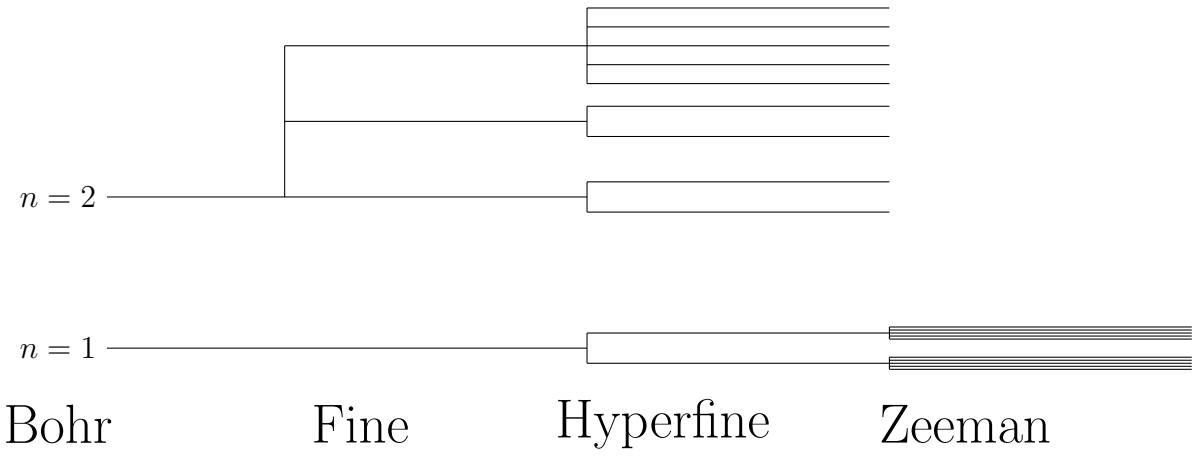

Figure 2.1: Figure of the splitting of energy levels due to the fine, hyperfine, and Zeeman structure. This figure isn't done yet; I'm going to work on it more.

degeneracy comes from the values of the z-component of the orbital angular momentum, $m_j = -F \dots F$. As we will see in the next section, the energy splitting due to the Zeeman effect will be quite important. Since sodium, the basis of LGS systems, live within the geomagnetic field, thereby splitting its energy levels. This turns out to have fascinating implications.

This is a lot to keep track of in our heads, but actually quite nice to look at diagrammatically. Figure 2.1 shows a schematic of the various structures. From left to right, the order of magnitude of the splitting gets smaller. As we move up vertically, we get progressively more splitting due to the higher levels of degeneracy as quantum numbers increase.

For sodium, the ground state is split into two levels, creating two distinct transitions, from $3p_{\frac{3}{2}}$ to 3s and $3p_{\frac{1}{2}}$ to 3s; these transitions have respective wavelengths 588.99 nm and 589.59 nm. The various energy levels of sodium are shown in Figure 2.2, with the transition from $3P \rightarrow 3S$ being used primarily in LGS. This transition, along with many others, is shown in Figure 2.2, with energy and wavenumber (inverse wavelength) plotted vertically.

2.2 Magnetic Resonant Pulsing

One technique that is often used in LGS to increase brightness is the usage of circularly polarized laser light. Photons can carry spin angular momentum (SAM), and due to conservation of angular momentum, this momentum is imparted to atom during absorption. When an atom absorbs a photon with SAM of $J = \pm\hbar$, the angular momentum of the atom must increase by the same amount, $\Delta m = +\hbar$. However, when the atom emits a photon, it can decay to any state satisfying

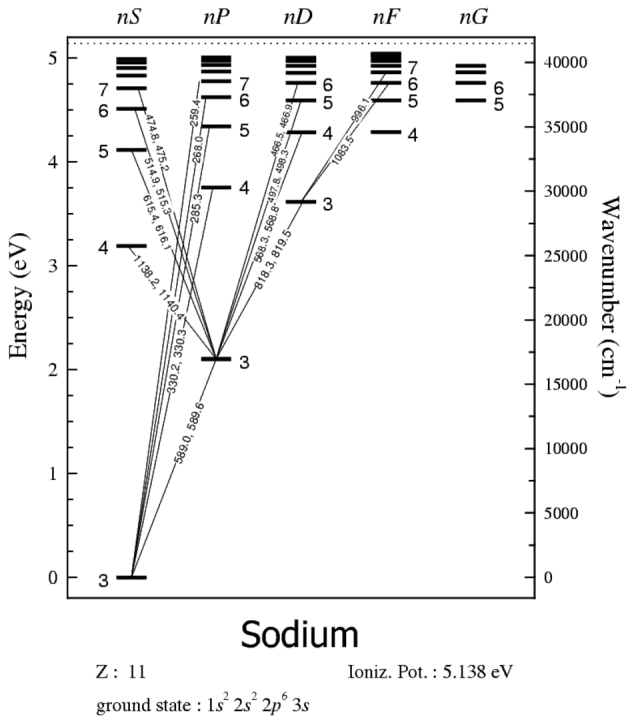

Figure 2.2: Figure of the energy levels of sodium, showing the possible transitions in energy the atom can make [Phy].

$\Delta m = \pm\hbar, 0$. However, the probability of decreasing angular momentum upon emission is significantly lower than a change of $\Delta m = 0, 1$. Hence, atoms tend to move towards states of higher angular momentum and eventually end up in a cyclical transition between the states of highest angular momentum. This process, shown in Figure 2.3, is known as *optical pumping* [TJK14]. Since the difference in energy between, for example, the $\frac{-3}{2} \rightarrow \frac{-1}{2}$ transition is different from the $\frac{3}{2} \rightarrow \frac{5}{2}$ transition, it is beneficial to have all atoms in the same state; this allows for the specific wavelength of light to precisely target this transition, increasing the probability of absorption. This can increase photon emission and absorption by a factor of 3 [Kib09].

However, when exposed to an external magnetic field, the $\vec{F}$ vector precesses about the magnetic field; this is known as *Larmor precession*. Classically, this precession can be thought due to the torque a magnetic field exerts on the atom:

$$\vec{\tau} = \vec{\mu} \times \vec{B} \tag{2.9}$$

where $\vec{\tau}$ is the torque on an atom with magnetic moment $\vec{\mu}$ in magnetic field $\vec{B}$. This equation can be rewritten by noting that the magnetic moment is the product of the gyromagnetic ratio and angular momentum of the atom:

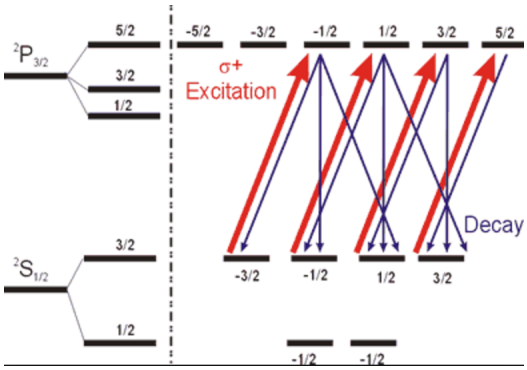

Figure 2.3: Figure of optical pumping in which the excitation of the atom results in an angular momentum change of $\Delta m = +1$ but decay governed by $\Delta m = \pm 1, 0$ [CER].

$$\vec{\mu} = \gamma \vec{J} \tag{2.10}$$

where $\vec{J}$ is the angular momentum and $\gamma = \frac{eg}{2m}$ is the gyromagnetic ratio with e being the charge of an electron, g being the g-factor,[5] and m being the mass of the atom. The toque can then be written as

$$\vec{\tau} = \gamma \vec{J} \times \vec{B}. \tag{2.11}$$

The angular frequency of this precession, known as the *Larmor frequency*, can be found by solving Equation 2.11, giving

$$\omega = \gamma B. \tag{2.12}$$

This precession can actually degrade the benefits obtained by optical pumping. Optical pumping relies on redistributing the angular momentum of the atom, but for a magnetic field not aligned with the direction of the laser beam, this redistribution now doesn't distribute angular momentum perfectly since the magnetic field reorients the $\vec{F}$. Typically, the magnetic field reorients the atom much faster than the benefits of optical pumping can be obtained [TJK14]. Thus, the increase in absorption and emission is greatly reduced for atoms exposed to a magnetic field.

However, let us return to our discussion of the Zeeman effect. We found that the energy shift due to the magnetic field is

[5]The g-factor, or g-value, is a dimensionless value that arises from a quantum treatment of the atom; it essentially accounts for the quantization of angular momentum of the nucleus.

$$\Delta E = \mu_0 m_j g_F B. \tag{2.13}$$

We can associate this energy difference with with a frequency of light by Equation 2.3, giving

$$f_Z = \frac{1}{h}\mu_0 m_j g_F B. \tag{2.14}$$

It turns out that the inverse of this frequency, $\frac{1}{f_Z}$ is the time at which an electron stays in an excited Zeeman state. Noting this, we can deduce a way to mitigate the negative effects that optical pumping encounters with exposure to magnetic fields. If we optically pump the atom with a laser that is pulsed with a repetition rate equal to f_Z, we will only be "talking" to the electrons when they are ready to be excited. This is known as *magnetic resonant pulsing*.

The above paragraph definitely needs some work. Open to suggestions!

The magnetic field is essentially cause the vector $\vec{F}$ to precess. Magnetic resonant pulsing can then be thought of giving the atom a kick of light at the same time every cycle, locking into a resonant mode.

2.3 Dye Lasers

Dye lasers were some of the first lasers to be used as laser guide stars. This is due a variety of factors: their wavelength can be precisely tuned over a broad spectral range, they are relatively cheap and easy to use, and they are fairly robust. In the modern age, many telescopes have opted for solid state and diode lasers with improved properties such as lower divergence and narrower linewidth. Nevertheless, dye lasers will be explained in this section because of their pedagogical importance and relevance to this project.

Laser is an acronym for *light amplification by stimulated emission of radiation*. In general, a laser consists of three parts: a pump, a medium, and a cavity. The pump provides enough energy to excite atoms in the medium into the excited state. The atoms then decay down into their ground state, releasing a photon in a random direction, known as spontaneous emission. However, if a spontaneously emitted photon comes into contact with another excited atom, it can cause that atom to decay and release a photon with the same direction and frequency it has; this is known as stimulated emission. If a cavity is created around the medium, possibly by placing mirrors on either side of the medium, photons will travel back and forth in the medium, stimulating the emission of more and more photons. These photons will continue to build, creating a powerful source of monochromatic, coherent light. One of the cavity mirrors can be made partially transmissive,

which will allow only a certain percentage of photons to pass through.This is the foundation of a laser.

A dye laser works in exactly the same way. Its medium is a fluid of florescent dye in a solvent, such as alcohol. The pump is commonly another laser with a frequency of light corresponding to the absorption wavelength of the dye molecules. The cavity can vary in design, but normally consists of a mirror at one end and a diffraction grating at the other [JES97].

The big advantage of dye lasers are their incredible tunability over a broad spectral range. This is a consequence of medium being dye molecules, which a relatively large chain molecule. Once excited by the pump, these molecules can relax in energy due to the many vibrational and rotational states they can reside in. These relaxations result in photons of varying wavelength being emitted spontaneously. In order to access and select these different wavelengths, a diffraction grating is placed at one end of the cavity. This allows the varying wavelengths to be split apart, and the desired wavelength can be chosen and sent back into the medium where it will stimulate the emission of more photons of equal wavelength. Dye lasers can typically have tunability over close to 100 nm [JES97].

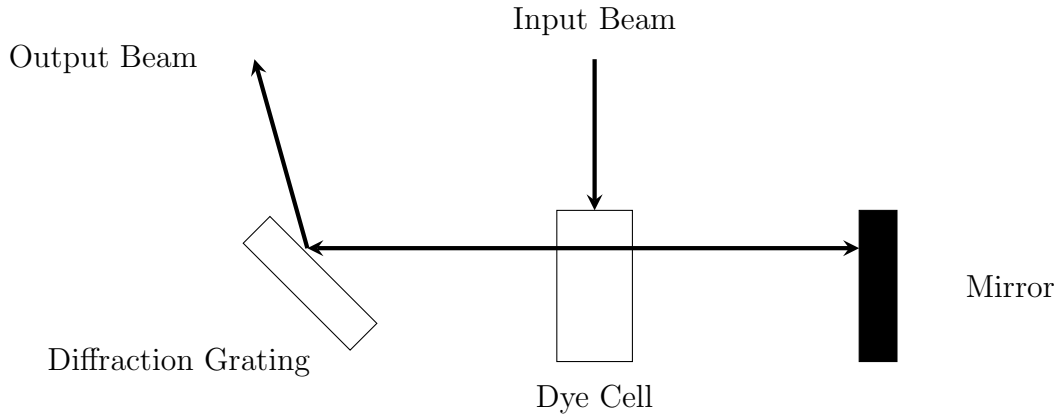

Figure 2.4: Schematic of a dye laser with dye fluid in the dye cell being pumped by a laser input beam and lasing in a cavity consisting of a mirror and diffraction grating.

A ultrashort dye laser, with pulse widths on the order of picoseconds and repetition rates of hundreds of kilohertz is significantly more difficult to construct than a CW or long pulse dye laser. In order to create a significant amount of stimulated emission, photons must have enough time to travel back and forth through the cavity a few times[6] to induce the stimulated emission of more photons from molecules in excited state. However, for ultrashort pulses, there is only a

[6]Technically, only one pass through the cavity is sufficient, but increasing to about 10 passes allows for a significant narrowing of the linewidth.

few picoseconds of interaction between the light and the molecules. Once the pulse has excited the molecules, they typically live in the excited state for a few nanoseconds [KS77]. In this time, the photons need to be able to pass ten times. The length of the cavity must then be on the order of

$$\begin{aligned} L &= \frac{1}{10} c\tau \\ &= \frac{1}{10} * 4 * 10^{-9} * 2.99 \times 10^{8} \\ &\approx 0.029\,\text{m}. \end{aligned} \tag{2.15}$$

where L is the total length of the lasing cavity, c is the speed of light, and τ is the pulse width. Experimentally, 3 cm is a pretty tight fit. Furthermore, because of the short interaction time between the pulse and the molecules, it is nontrivial to wonder whether enough molecules are being excited by the pulse in order to produce a output of laser light.

2.4 Second Harmonic Generation

A common laboratory laser is the neodymium doped solid state laser, such as the Nd:YAG or Nd:$V0_4$. These lasers excite rods of neodymium with a flash lamp, producing pulses of light in the infrared at $\lambda = 1063\,\text{nm}$. However, most dyes are resonant in the visible, typically around $\lambda = 532\,\text{nm}$. Thus, we need to convert 1064 light into 532.

The harmonic field of a wave can be described by

$$E_i = \varepsilon_i e^{-i\omega t} \tag{2.16}$$

where ε is the amplitude of the field, ω is the frequency, and t is a time dependence [dD06]. For a linear crystal, the polarization can be described by a linear function

$$\vec{P} = \epsilon_0 \chi^{(1)} \vec{E} \tag{2.17}$$

where ϵ_0 is the permittivity of free space, $\chi^{(1)}$ is the linear electric susceptibility[7] and $\vec{E}$ is the induced electric field. The polarization is thus the electric field multiplied by a constant.

[7]The linear electric susceptibility is a constant that relates polarization inside a medium to the induced electric field; it is given by $\chi = \epsilon_r$ where ϵ_r is the dielectric constant. Thus, in a vacuum where $\epsilon_r = 1$, we can see $\chi = 0$.

However, things get much more interesting when we introduce a nonlinear crystal. This type of crystal has a nonlinear polarization function. Using a Taylor expansion, we can write this polarization as

$$\vec{P} = \epsilon_0 \left(\chi^{(1)}_{ik} E_i + \chi^{(2)}_{ijk} E_i E_j + \chi^{(3)}_{ijlk} E_i E_j E_l + \dots \right) \tag{2.18}$$

where each $\chi^{(n)}$ represents the tensor of the n^{th} susceptibility and the notation $\chi_{ik} E_i$ corresponds to an Einstein summation.[8] If we now substitute in out electric field from Equation 2.16, we see that we will get terms of order E^2. If we look specifically at the polarization for these second order terms, we find

$$P_k = \epsilon_0 \left(\varepsilon_i \varepsilon_j e^{-2i\omega t} + \varepsilon_i^* \varepsilon_j^* e^{2i\omega t} + \varepsilon_i^* \varepsilon_j + \varepsilon_i \varepsilon_j^* \right). \tag{2.19}$$

Thus, we see terms of $e^{2i\omega t}$, implying that not only do we have the linear field with frequency ω, but we have picked up a field with frequency 2ω [dD06]. For most high power lasers, the second-order term dominates, implying a majority of light is frequency doubled by the nonlinear term and a negligible amount of light passes through without being doubled.

This is second harmonic generation, or frequency doubling. It is a process that occurs in nonlinear crystal where a photon of frequency f_1 is converted into to photons each of frequency f_2 with $2f_1 = f_2$. Since, the energy of a photon is linearly proportional to its frequency, this makes intuitive sense from a conservation of energy perspective. A depiction of this is shown in Figure 2.5, where the initial light is known as the fundamental wave and frequency doubled light is known as the second harmonic wave..

This process occurs because of the *birefringence* of the crystal. Birefringence is the property of a material having different refractive indices based upon the polarization of the incoming light; this is unique since for most materials, the index of refraction is uniform and dependent only upon the wavelength of light. For birefringent materials, their exists two different indices of refraction; each of these indices occur when the polarization is parallel to a specific axis within the crystal. These two axes are known as the *ordinary* axis and the *extraordinary* axis; light with polarization along the ordinary axis will follow the standard rules of refraction (hence the name ordinary), given by Equation A.1. However, light with polarization along the extraordinary with a different index of refraction and travel at a speed different from the light with ordinary polarization.

In order to achieve maximum efficiency during a frequency doubling conversion, we need the phase difference between the fundamental and second harmonic to be approximately zero

[8] Einstein notation is a shorthand way of writing summations. For any repeated indices, we compute a summation of each index; for example, $\chi_{ik} E_i = \sum_{i=1} \chi_{ik} E_i$.

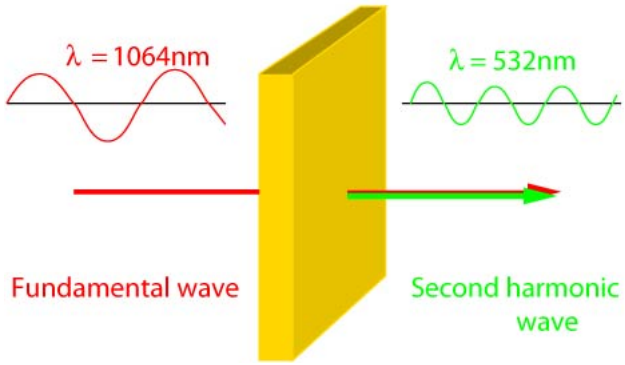

Figure 2.5: Depiction of second harmonic generation where an incoming photon is converted into two photons, each with twice the frequency as the initial photon [SHG].

$$\Delta k = k_1 + 2k_2 \tag{2.20}$$

where Δk is the phase difference, k_1 is the phase of the fundamental wave, and k_2 is the phase of the second harmonic. This is shown qualitatively in Figure 2.6. Having a phase difference of $\Delta k = 0$ ensures that no destructive interference between the waves will occur, resulting in maximum output power.

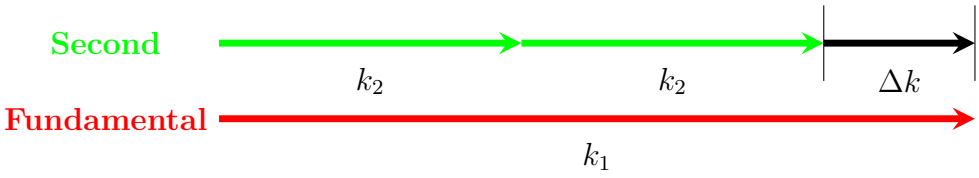

Figure 2.6: Figure showing the phase matching of the fundamental and second harmonic wave. In order to achieve maximum efficiency, $\Delta k \approx 0$.

Thus, by using a second harmonic generation crystal, we can convert 1064 nm into 532 nm, which will be capable of exciting the LDS-798 dye in our dye laser. These crystals are typically very sensitive to many parameters, including orientation with respect to the laser beam, angle with respect to the laser's polarization, and temperature.

3 Laser System

3.1 Duetto Laser

rep rate, pulse length, power, energy, about

3.2 Second Harmonic Generation

crystal, properties, data about resistance and conversion eff.

I have figure to put in here: resistance vs temperature resistance vs current efficiency vs temperature

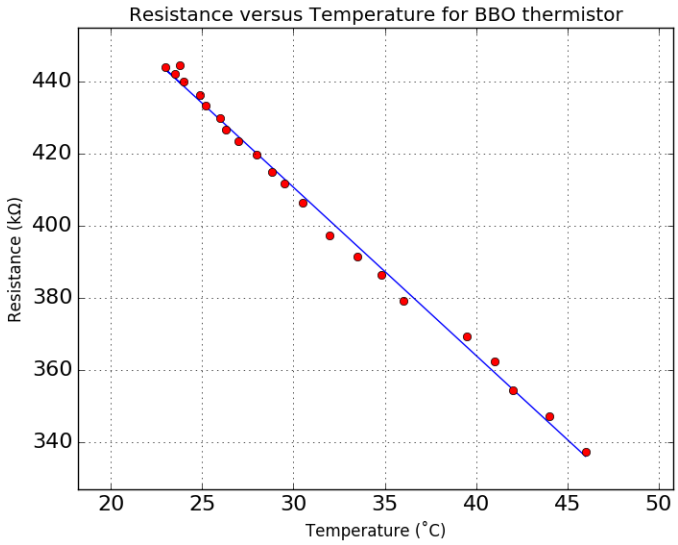

Figure 3.1: rvt

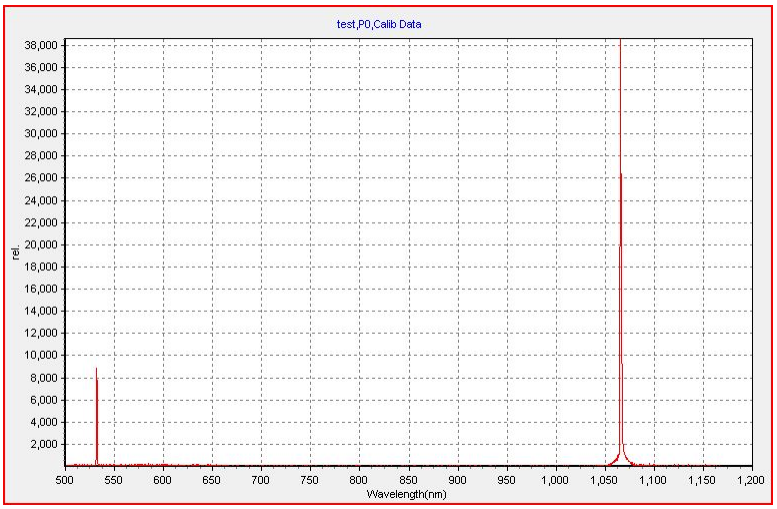

Figure 3.2: Conversion spectrum

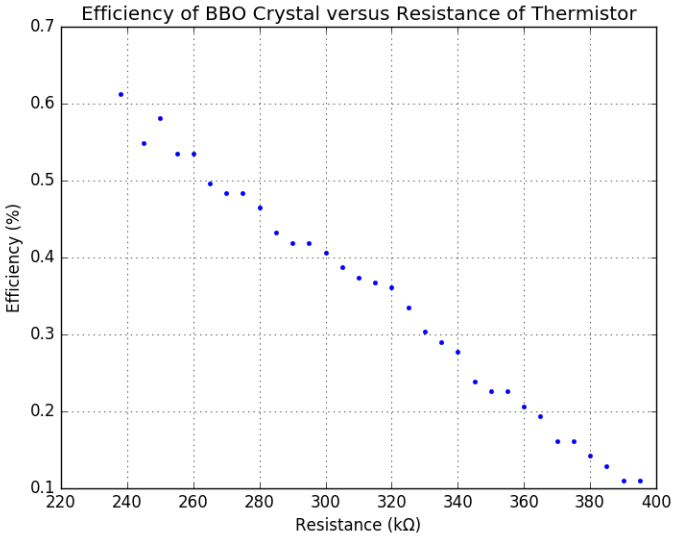

Figure 3.3: efficiency of crystal

3.3 Dye Laser Cavity

Critical length, methods of alignment, dual pumping? Wavelength and tunability, spectra

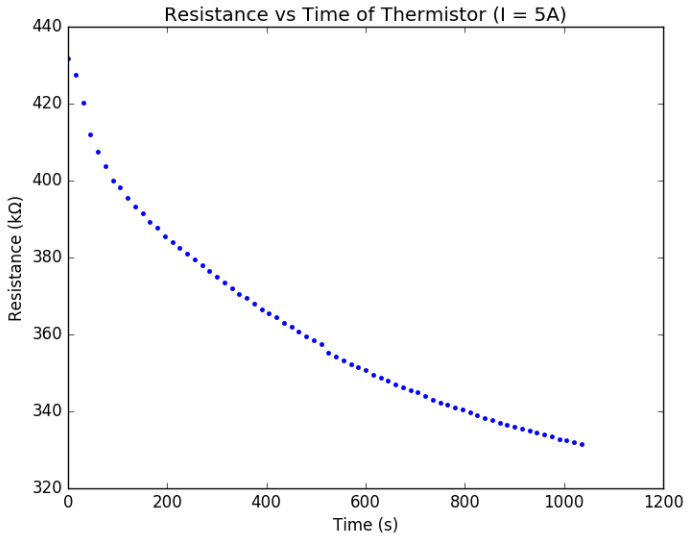

Figure 3.4: Fluctuations in resistance

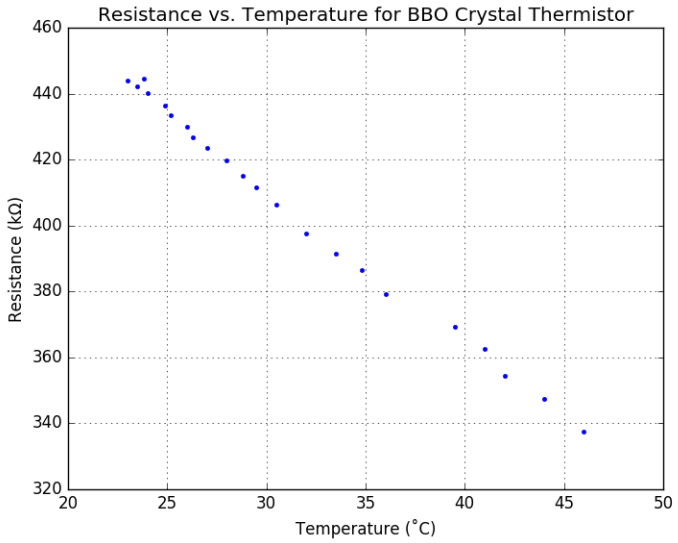

Figure 3.5: Resistance versus temperature of thermistor

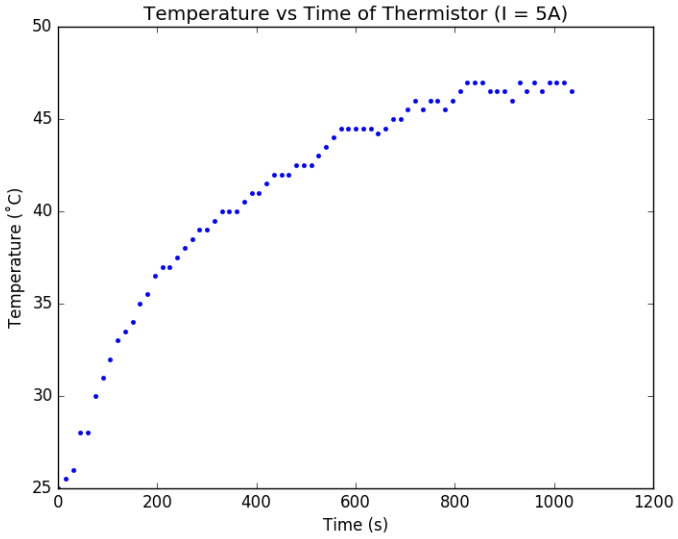

Figure 3.6: Temperature fluctuations of thermistor

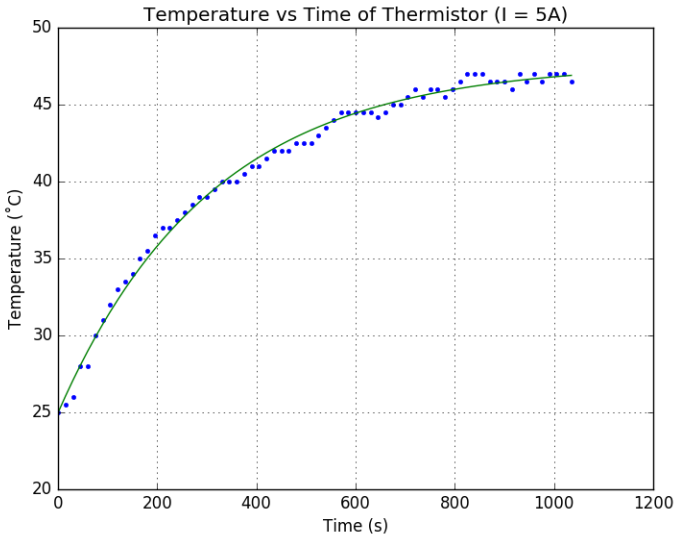

Figure 3.7: Best fit of the temperature fluctuations

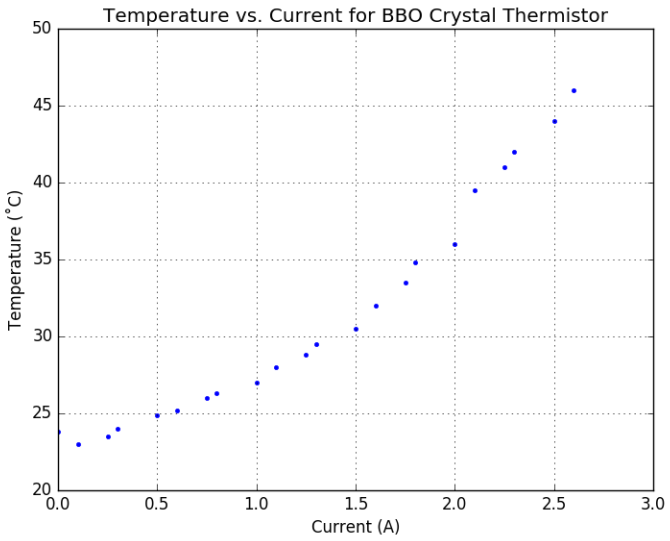

Figure 3.8: Temperature versus current for transistor

4 Magnetic Field Housing

Calculate gyromagnetic ratio, larmor frequency, magnetic field required, current required, geometry, testing, magnetic field data, homogeneity stability

5 Absorption Spectroscopy

absorption spectroscopy of rubidium with pulsed dye laser. Show difference in absorption (or no difference) when repetition rate is equal to that of the larmor precession (determined by magnetic field)

6 Conclusion

Conclude everything, did it work, did it not work, where should people go next, what is the significance

A Laser Guide Stars

Telescopes observing distant astronomical objects face a significant challenge known as atmospheric distortion. Light coming from these objects travels in a straight line with little obstruction in the near vacuum of space. However, as this ray of light travels from free space into the atmosphere of Earth, it is affected by the many gaseous particles that make up the atmosphere. The effect is a bending of the light rays, known as *refraction*, and can be described mathematically by Snell's Law,

$$n_1 \sin\theta_1 = n_2 \sin\theta_2 \tag{A.1}$$

where n_1 is the index of refraction of the first medium, n_2 is the refractive index of the second medium, and θ_1 and θ_2 are the angles that the ray makes with the normal to the medium; a schematic of this is shown in A.1.

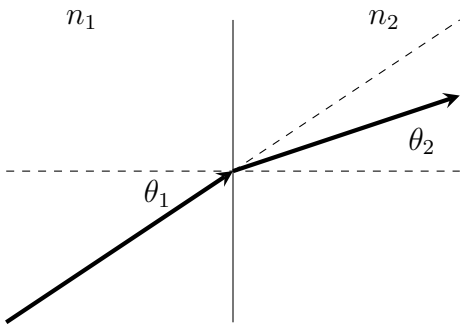

Figure A.1: Schematic of a ray of light refracting according to Snell's Law as it passes from medium of refractive index n_1 into a medium with refractive index n_2.

In general, the many light rays that make up the observed object will be refracted uniformly causing the object to be perceived in a location that is different from its true position. However, if we look closer, we find that the atmosphere

does not refract all light rays in the same manner, but small variations in pressure, temperature, and density cause a change in the index of refraction at that specific location, causing light rays that are close together to be refracted in slightly different ways; this is known as *atmospheric distortion*. A schematic is shown in Figure A.2, with plane waves being distorted as they pass through an atmosphere.

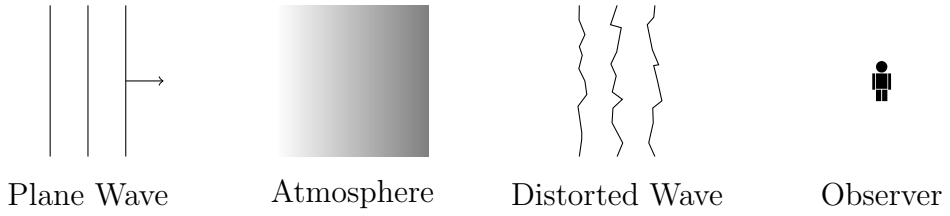

Figure A.2: Atmospheric distortion of a plane wave passing through Earth's atmosphere

The idea of atmospheric will be familiar to those who have seen the sunset on the horizon. As the sun nears the horizon, the light is bent strongly through the atmosphere, picking much more distortion than when high in the sky. This results in a disfiguring of its spherical shape and a sharpening around the edges. An image of this is shown if Figure A.3.

In order for telescopes then to improve resolution, astronomers need to find a way to rid their systems of this atmospheric distortion. One way to do this is to place the telescope outside of Earth's atmosphere where it would be unaffected by atmospheric distortion, which was done with amazing success in 1990 with the low-orbiting, powerful Hubble telescope. However, it is not only extremely costly to put telescopes into orbit, but also difficult pragmatically as they cannot be easily maintained or serviced.

Thus, a different solution was proposed. If astronomers could model how exactly the light was distorted as it passed through the atmosphere, they could subtract those distortions from their images and obtain better data. In order to measure the amount of distortion, the telescope can observe a point source in the sky, such as a distant star, and observe its image. This is then compared with how a point source would be imaged through the telescope without atmospheric distortion, and the difference between the two gives the amount of distortion. This process is known as *adaptive optics*, and more information is given in Appendix B.

However, there are not always stars bright enough in the telescope's field of view that can be used as the point source, or guide star [PW06]. In order to skirt this problem, artificial stars were constructed, known as *laser guide stars*. A laser guide star is created by sending laser light into the atmosphere, where it interacts

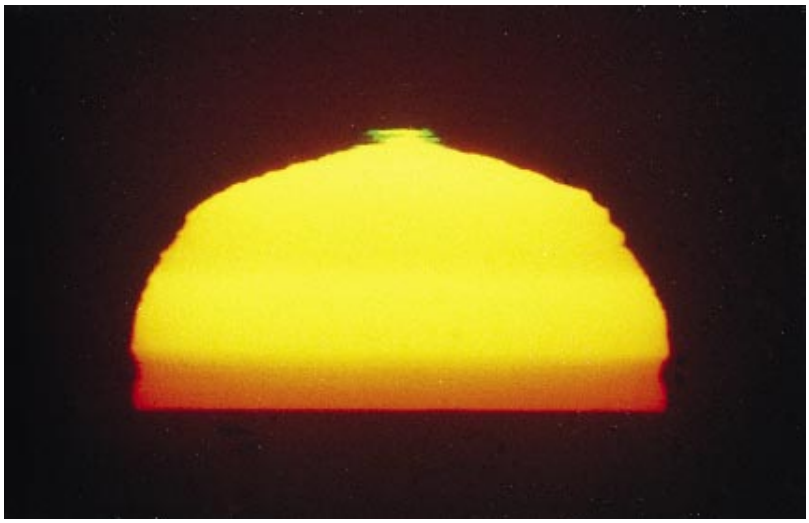

Figure A.3: Image of a sunset, with atmospheric distortion disfiguring the spherical shape of the sun and creating sharp patterns on the edges [ST].

with a layer of sodium atoms.[1] Using a laser with a wavelength resonant with sodium, the atoms will absorb and emit this laser light, creating a glowing sphere in the upper atmosphere, as described in Chapter 2. This sphere of light is then used as the guide star.

In general, most large-scale, ground-based telescopes now have powerful lasers with wavelengths precisely tuned to be resonant with sodium. While these telescopes are making observations, the lasers are shone into the sky to create the LGS; an image of a LGS being created is shown in Figure A.4. The LGS is observed and atmospheric distortions are calculated and subtracted from the image in real time.

One major concern for LGS systems is their brightness in the sky [PW06]. It is important for the star to be bright enough that the telescope system is able to pick up enough light for measurement of the distortion. The shape of the LGS is also important, as it must be as near to circular as possible in order for an accurate measurement of the distortion to be made. The shape of the LGS is mostly due to the profile of the laser beam [RH10], and won't be discussed here.

In order to create a brighter laser guide star, a few methods are utilized. One method is to increase the intensity, the power per unit area, of the laser. This will allow for more atoms to absorb and emit light, thereby creating a brighter

[1] Approximately 60 km in the atmosphere lies a 10 km thick layer of sodium atoms. These atoms come from meteorites as they burn up in Earth's atmosphere, leaving behind their composite particles, a significant portion being sodium metal [Kib09]. The density of this sodium layer varies throughout a given day and throughout the year, but typically is near 5×10^{13} atoms/m^2 [Kib09].

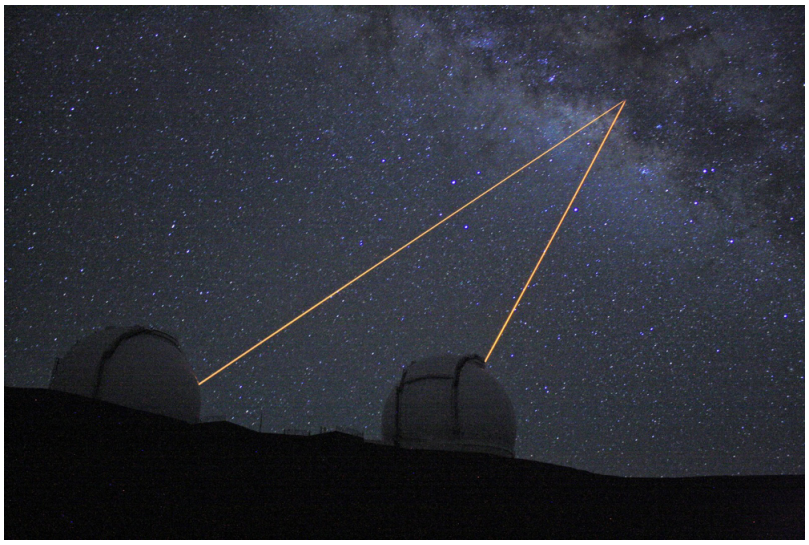

Figure A.4: Image of a laser guide star being created at the Very Large Telescope [Uni].

star. Another method is to increase the diameter of the laser beam, which will allow for a greater area of sodium atoms to be reached by the light. A more sophisticated method, which is detail in Chapter 2, known as optical pumping, makes use of circularly polarized light to exploit a quantum mechanical state of the atom's energy levels. The method explored in this paper takes advantage of the geomagnetic field, the Zeeman effect, and a pulsed laser to increase the brightness of LGS.

B Adaptive Optics

The process of measuring the atmospheric distortion in order to enhance astronomical imaging, known as *adaptive optics*, turns out to be quite tricky. Here we present an introduction to the methods used during this process.

In general, telescopes observe the LGS and the astronomical object simultaneously. Theimage of the LGS is then compared to an ideal point source imaged through the telescope, and the distortion is calculated by comparing these two. A deformable mirror, composed of many smaller mirrors each of which can moved precisely, and is then used to create the opposite of the calculated distortion. The image of the astronomical object is then reflected off this mirror, thereby ridding the image of distortion.

In order to calculate the atmospheric distortion, astronomers make use of the well defined way in which point sources are imaged through optical systems. When an idealized point in imaged through an optical system, it has a certain energy distribution in image space, known as the point spread function. For an optical system with spherical symmetry and no aberration, the point spread function can be described mathematically along one coordinate as

$$P(x) = \frac{J_1(x)}{x} \tag{B.1}$$

where $J_1(x)$ is the Bessel function of first kind. This function is known as the Airy Disk and is shown in Figure B.1; it is an idealized description of a point imaged through a perfect optical system.

It turns out that stars are very close to being idealized point sources and can thus be used as this idealized point source. Since the light from these stars is passing through Earth's atmosphere, it will be distorted and these distortions will show up in the point spread function, thus deviating from the Airy Disk described by Equation B.1.

Astronomers then use a combination of Fourier mathematics and an optimization algorithm to calculate the distortion; this method follows that outlined by Gonsalves [Gon82]. The phase of the distortion can be described as a summation:

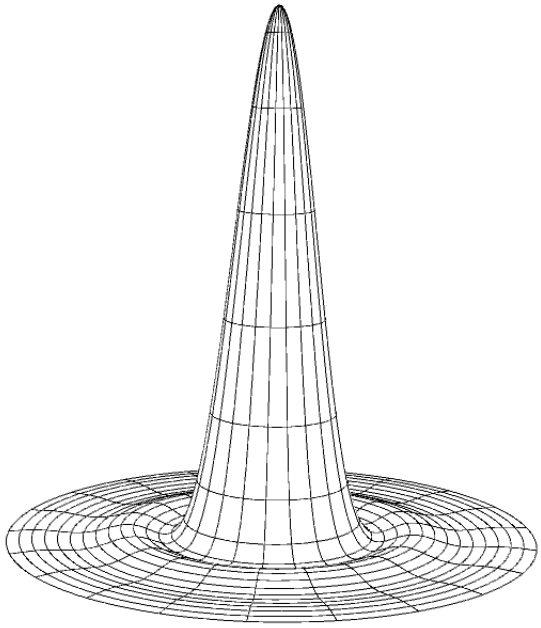

Figure B.1: Graph of the Airy Disk function, describing an idealized point imaged through a spherically symmetric, aberration free optical system

$$\theta(\omega) = \sum_{k=0}^{\infty} c_k \phi(\omega) \tag{B.2}$$

where $\{\phi(\omega)\}$ is a set of polynomials and c_k is a coefficient that quantifies how much of each polynomial is present in the distortion. This phase can then be used to create a point spread function that would model a system with that certain distortion. This is done by first calculating optical transfer function

$$H(\omega) = A(\omega)e^{i\theta(\omega)} \tag{B.3}$$

where $A(\omega)$ is the aperture function[1] of the system and $\theta(\omega)$ is the phase described above. Taking the inverse Fourier transform and then the modulus squared, we arrive at the point spread function

$$P(x) = \left| ifft[H(\omega)] \right|^2 \tag{B.4}$$

[1]The aperture function is normally a function describing where light can and cannot pass through. For a circular aperture, it would consist of a solid circle where light can pass through and nothing around the circle indicating light out here does not show up in the point spread function.

where $ifft$ denotes the inverse Fourier transform of the argument. Thus, while taking observations can also observe the distorted point spread function of a star, a computer iterates through many different polynomials until the estimated point spread function is similar to the observed point spread function, and then an estimate of the phase of the distortion is known [RQF91].

Searching for the correct polynomials weighted by the correct coefficients is not trivial. Sometimes certain polynomials can be ignored if it known by symmetry that they will not show up in the point spread function. Regardless, searching for the correct distortion is an optimization of a function in a huge parameter space. Typical algorithms use a steepest descent approach, which changes one parameter at a time, calculates an error between that estimation and the observed point spread function, and seeks to minimize this error. There have also been algorithms that use random searches, Monte Carlo walks, and Markov chain Monte Carlo searches that claim robustness and speed.

Once the correct distortion is calculated, the information is sent to the deformable mirror, which is where the term "adaptive optics" comes from. This mirror is made up of many smaller mirrors, each of which is precisely movable by a piezoelectric motor. The mirror changes shape, creating a conjugate wavefront that the image from the telescope can be reflected off. At this point, the atmospheric distortion has been removed from the image. Normally, this is done in real time, and so speed of both the calculation algorithm and of the deformable must be optimized. Systems typically can calculate and adjust in under a second.

An example of this is the time independent problem of reducing an unknown aberration in an optical system. Say, for example, you bought a huge lens for your telescope. You set it up, and look at Venus, but upon looking at it, you realize that while the center of Venus is in focus, the edge is out of focus, or vice versa. You deduce that your new lens has spherical aberration (thanks to the manufacturer)! However, you need to collect data and a new lens won't be ready in time. Miraculously, you have a deformable mirror lying around, and decide to try your hand at adaptive optics.

You then find a nice star and take a picture of it with your telescope. Using the Zernike polynomials described in Equation B.5, which describe most common aberrations in typical optical system; you calculate the Z_4^0 Zernike polynomial corresponding to spherical aberration.

$$\begin{aligned} Z_n^m(\rho,\phi) &= R_n^m(\rho)\cos(m\phi) \\ Z_n^{-m}(\rho,\phi) &= R_n^m(\rho)\sin(m\phi) \\ R_n^m(\rho) &= \sum_{k=0}^{\frac{n-m}{2}} \frac{(-1)^k(n-k)!}{k!(\frac{n+m}{2}-k)!(\frac{n-m}{2}+k)} \end{aligned} \tag{B.5}$$

From here, you create a point spread function with varying amounts of spherical aberration by weighting this Z_4^0 by different amounts. The algorithm doesn't take too long, since you only have one parameter to tune. Once you get a point spread function similar to the one of the observed star, you declare you have found the aberration in your lens! You then create this distortion in your deformable mirror, reflect the image of Venus off of this mirror, and collect your data.

Bibliography

[Bra00] U. Brackmann, *Lambdachrome laser dyes*, Lambda Physik **3rd Edition** (2000).

[CER] CERN, *Spin polarization by optical pumping*, `https://collaps.web.cern.ch/beta-nmr/spin-polarization`, Accessed: 12.11.2017.

[dD06] M.J.A de Dood, *Second-harmonic generation: how to get from a wavelength of 980 to 490*, Huygens Laboratory (2006).

[Fey65] Richard Feynman, *The hyperfine splitting in hydrogen*, California Institute of Technology (1965).

[Gon82] R. A. Gonsalves, *Phase retrieval and diversity in adaptive optics*, Optical Engineering **21.5** (1982), 829 – 832.

[JES97] S. G. Payton J. E. Sohl, *A modular, reconfigurable cavity, pulsed dye laser for the advanced undergraduate laboratory*, American Journal of Physics **65.7** (1997), 640–652.

[JH01] A. Gregory J. Henry, *Moving heaven and earth: Copernicus and the solar system*, Cambridge (2001), 87.

[Kib09] E. Kibblewhite, *The physics of the sodium laser guide star: Predicting and enhancing the photon returns*, Advanced Maui Optical and Space Surveilance Technologies Conference (2009).

[KS77] T. Sikkeland K.A. Selanger, J. Falnes, *Flourescence lifetime studies of rhodamine 6g in methanol*, The Journal of Physics Chemistry **81.20** (1977), 1960–1963.

[NAS03] NASA, *Telescope history*, `https://www.nasa.gov/audience/forstudents/9-12/features/telescope_feature_912.html`, 09.12.03, Accessed: 12.11.2017.

[Obs09] W. M. Keck Observatory, *A short history of astronomy and telescopes*, 2009.

[Phy] Raptor Physics, *Energy level diagrams*, `http://raptor.physics.wisc.edu/download2.htm`, Accessed: 14.11.2017.

[PW06] A. H. Bouchez R. D. Campbell J. C. Y. Chin A. R. Contos M. A. van Dam S. K. Hartman E. M. Johansson R. E. Lafon P.L. Wizinowich, D.L. Mignant, *The w.m. keck observatory laser guide star adaptive optics system: Overview*, Astronomical Society of the Pacific **118** (2006), 840.

[RH10] D. Bonaccini Calia D. Budker J. M. Higbie W. Hackenberg R. Holzlohner, S. M. Rochester, *Optimization of cw sodium laser guide star efficiency*, Astronomy and Astrophysics **510** (2010).

[RQF91] D. L. Fried R. Q. Fugate, *Measurement of atmospheric wavefront distortion using scattered light from a laser guide-star*, Nature **353** (1991), 6340.

[RR10] S. M. Rochester R. Holzlohner R. Rampy, D. Gavel, *Optimization of cw sodium laser guide star efficiency*, Astronomy and Astrophysics **510** (2010), A20.

[SHG] *Second harmonic generation*, `https://staff.aist.go.jp/narazaki-aiko/SHG`, Accessed: 16.11.2017.

[ST] Sky and Telescope, *How to successfully beat atmospheric distortion*, `http://www.skyandtelescope.com/astronomy-equipment/beating-the-seeing/`, Accessed: 15.11.2017.

[TJK14] C. A. Denman T. J. Kane, P. D. Hillman, *Pulsed laser architecture for enhancing backscatter from sodium*, SPIE **9148** (2014), 3G.

[Uni] Penn State University, *Not just a laser pointer*, `http://sites.psu.edu/howzenscienceofmovies/2014/10/03/not-just-a-laser-pointer/`, Accessed: 15.11.2017.